Temperature Dependence of the Relative Rates of Chlorination and Hydrolysis

of N2O5 in NaCl-Water Solutions

Steven J. Kregel,¹ Thomas F. Derrah,¹ SeokJin Moon,² David T. Limmer,^{2,3,4,5*}
Gilbert M. Nathanson,^{1*} and Timothy H. Bertram^{1*}

⁵ Material Sciences Division, Lawrence Berkeley National Laboratory, Berkeley, CA, 94720, USA

Abstract

We have measured the temperature dependence of the ClNO₂ product yield in competition with hydrolysis following N₂O₅ uptake to aqueous NaCl solutions. For NaCl-D₂O solutions spanning 0.0054 to 0.21 M, the ClNO₂ product yield decreases on average by only 5% from 5 to 25 °C. Less reproducible measurements at 0.54 and 2.4 M NaCl also fall within this range. The ratio of the rate constants for chlorination and hydrolysis of N₂O₅ in D₂O is determined to be 1147 \pm 65 at 25 °C, favoring chlorination. An Arrhenius analysis reveals that the activation energy for hydrolysis is just 3.0 \pm 1.8 kJ/mol larger than for chlorination. In combination with the measured pre-exponential ratio favoring chlorination of 419 $^{+542}_{-215}$, we conclude that the strong preference of N₂O₅ to undergo chlorination over hydrolysis is driven by dynamic and entropic, rather than enthalpic, factors. Molecular dynamics simulations elucidate the distinct solvation between strongly hydrated Cl⁻ and the hydrophobically solvated N₂O₅. Combining this molecular picture with the Arrhenius analysis implicates the role of water in mediating interactions between such distinctly solvated species and suggests a role for diffusion limitations on the chlorination reaction.

Contact Information: Timothy Bertram: timothy.bertram@wisc.edu, Gilbert Nathanson: nathanson@chem.wisc.edu,

¹ Department of Chemistry, University of Wisconsin-Madison, Madison, WI, 53706, USA

² Department of Chemistry, University of California, Berkeley, CA, 94720, USA

³ Kavli Energy NanoScience Institute, University of California, Berkeley, CA, 94720, USA

⁴ Chemical Sciences Division, Lawrence Berkeley National Laboratory, Berkeley, CA, 94720, USA

INTRODUCTION

Dinitrogen pentoxide (N_2O_5) is a nocturnal reservoir of NO_x ($NO_x \equiv NO + NO_2$) in the atmosphere. Reactions of N_2O_5 with aqueous aerosol particles comprise a major sink for NO_x , with consequent effects on tropospheric ozone production.^{1,2} The heterogeneous uptake of N_2O_5 to aerosol particles can result in hydrolysis to produce NO_3^- and H^+ (R1) and chlorination to produce nitryl chloride (ClNO₂) in the presence of Cl^- (R2):

$$N_2O_5(g) + H_2O \rightarrow 2NO_3^- + 2H^+$$
 R1

$$N_2O_5(g) + Cl^- \rightarrow ClNO_2(g) + NO_3^-$$
 R2

Due to its limited solubility, ClNO₂ rapidly evaporates from aerosol particles, where it photolyzes to produce Cl radicals and regenerate NO₂.³ In urban environments, Cl radicals can efficiently oxidize volatile organic compounds, leading to tropospheric ozone production.^{3,4} On a global scale, the efficient removal of NO_x from the reactive uptake of N₂O₅ reduces the atmospheric abundance of O₃ and OH, which in turn extends the lifetime of CH₄.⁵ The production of H⁺ and NO₃⁻ from the hydrolysis of N₂O₅ results in acidification and nitrification of aerosols, which has been shown on the regional scale to contribute to particulate matter air quality exceedance events.^{6,7}

Previous laboratory experiments have focused on investigating the production of ClNO₂ as a function of solution-phase chloride and added ions and surfactants. ^{8–13} Behnke *et al.* measured the production of ClNO₂ over bulk solutions and found that at high chloride concentrations (i.e., [Cl⁻] > 2M) ClNO₂ was the only product observed. ⁸ Bertram and Thornton developed a parametrization for the total reactive uptake of N₂O₅ as a function of water, nitrate, and chloride concentrations in aqueous aerosols, and found that small concentrations of chloride reversed the inhibition of N₂O₅ reactive uptake induced by high dissolved nitrate concentrations. ⁹ Their findings confirmed the results of Behnke *et. al.* that ClNO₂ is the primary reaction product in the presence of high [Cl⁻], and implied that ClNO₂ is much less reactive in aerosols than N₂O₅. Roberts

et. al. investigated the production of CINO₂ at lower concentrations of chloride and determined the ratio of rate constants for the chlorination (k_{Cl^-}) and hydrolysis (k_w) reactions.¹¹ Due to their large observed rate constant ratio, 450 ± 100 , they postulated that the activation energy for hydrolysis is significantly larger than for chlorination, implying that chlorination would be favored at lower temperatures. It has also been shown that non-chloride anions (such as sulfate and acetate) suppress the production of CINO₂, most likely through S_N2 reactions that outcompete Cl⁻ attack, forming short-lived intermediates that ultimately decompose via hydrolysis.^{10,13} Ryder et. al. found that reactive seawater surfactants can drastically decrease CINO₂ production; model studies using phenol, a surface-active aromatic, indicate that its nitration by N₂O₅ preferentially occurs within the top few monolayers, again outcompeting the less interfacially abundant Cl⁻ ion.¹² Charged surfactants may also impact the production of CINO₂ by altering the depth profiles of chloride anions in the interfacial region.¹⁴ Field studies support the role of processes like these in reducing the fraction of CINO₂ produced from N₂O₅.^{13,15}

Existing studies do not provide evidence for a systematic dependence of the reactive uptake of N₂O₅ on chloride concentration to within the uncertainty of measurements, which are centered around reaction probabilities between 0.01 and 0.04.8,16–21 This observation is consistent with the assumption that the rates of N₂O₅ reactions are limited by the dissociation of N₂O₅ into NO₂⁺ and NO₃⁻, followed by subsequent reaction of NO₂⁺ with water or solute anions.²² Roberts *et. al.* rationalized their proposed temperature dependance on the ClNO₂ yield via this mechanism by invoking a barrierless reaction between the oppositely charged NO₂⁺ and Cl⁻ reactants versus a more significant barrier for the ion-neutral reaction of NO₂⁺ with H₂O.¹¹

However, recent theoretical $^{23-28}$ and laboratory 9,18 studies have called into question the existence of isolated aqueous NO_2^+ ions. Bianco and Hynes first proposed concerted hydrolysis

involving nucleophilic OH^{δ^-} attack from H_2O on molecular $NO_2^{\delta^+}NO_3^{\delta^-}$ that has incipient ion-pair character. This suggestion was elaborated by McNamara and Hillier through quantum chemistry calculations of $N_2O_5(H_2O)_n$ that corroborated the intact nature of N_2O_5 , both for hydrolysis (n = 0-6) and for CI^- attack (n = 0-1). Using *ab initio* molecular dynamics, Rossich Molina and Gerber further discovered that N_2O_5 may undergo hydrolysis on the surface of an $(H_2O)_{20}$ cluster by either nucleophilic (70%) or electrophilic (30%) attack of $H^{\delta^+}OH^{\delta^-}$ on $NO_2^{\delta^+}NO_3^{\delta^-}$. Most recently, Galib and Limmer and separately Cruzeiro, Galib, Limmer, and Götz employed molecular simulations and reaction-diffusion models to explore hydrolysis in the vicinity of an extended liquid-vapor interface. These studies reveal that N_2O_5 undergoes hydrolysis within the top 20 Å of solution, with up to 20% of hydrolysis occurring at the interface itself. The lifetime of $NO_2^{\delta^+}$ from dissociating $NO_2^{\delta^+}NO_3^{\delta^-}$ is found to be on the picosecond timescale as it is attacked by $H^{\delta^+}OH^{\delta^-}$. Karimova and Gerber have also shown that $NO_2^{\delta^+}NO_3^{\delta^-}$ in a $(H_2O)_{12}$ complex can undergo S_N2 attack by CI^- as NO_3^- concertedly departs, a mechanism that is distinct from S_N1 attack on solvent-separated $NO_2^{\delta^+}I^{0,30}$

Based on the theoretical predictions described above, we replace attack of H₂O or Cl⁻ on pre-existing NO₂⁺ with attack on NO₂δ⁺NO₃δ⁻ in our analysis. We may still expect a significant temperature dependence for the competition between R1 and R2 because chlorination requires only bond breaking within N₂O₅ and involves an anion approaching a charge-fluctuating molecule. In contrast, hydrolysis involves concerted bond breaking in both H₂O and N₂O₅ reactants as density fluctuations bring them together. The thousand-fold higher rate constant for chlorination over hydrolysis may arise from a larger energetic barrier for this dual bond breaking pathway between overall neutral reactants.

This study addresses the nature of R1 and R2 by directly measuring the competition between hydrolysis and chlorination over temperatures from 5 to 25 °C at chloride concentrations from 0.0054 to 2.4 M NaCl. This temperature span was chosen to reflect the conditions present in the lower troposphere where the majority of N₂O₅ heterogeneous uptake occurs, and the concentration range was chosen to provide ClNO₂ product yields ranging from a few percent to nearly complete conversion to ClNO₂, as shown in previous studies.^{8,11–13} The key quantity that we measure is the ClNO₂ product yield, or branching between R1 and R2, equal to the fraction of reacting N₂O₅ that produce ClNO₂. To our surprise, we measure only a small temperature dependence, suggesting that a single set of temperature independent ClNO₂ product yields may suffice in atmospheric modeling of hydrolysis and chlorination. An Arrhenius analysis enables us to further explore the fundamental competition between solute-solute and solute-solvent reactions, in this case involving solute Cl⁻ and solvent water attack on N₂O₅. This analysis reveals that the activation energy for hydrolysis is only 3.0 ± 1.8 kJ/mol higher than for chlorination. This small activation energy (equal to 1.2 RT at 25 °C) implies that the larger rate constant for chlorination over hydrolysis is not driven enthalpically, but rather through a combination of entropic and dynamic effects. With molecular simulations, we can quantify changes in solvent water coordination as the ionic and neutral reactants find each other in solution and use these calculations with diffusion-limited kinetic theory to gain insight into the chlorination rate.

EXPERIMENTAL PROCEDURE

The product yield of ClNO₂ following reactive uptake of N₂O₅ to NaCl solutions with concentrations of 0.0054, 0.014, 0.026, 0.055, 0.099, 0.21, 0.54, and 2.4 M was measured at 5, 10, 15, 20, and 25 °C using an approach based on Roberts *et. al.*¹¹ and Staudt *et. al.*¹³ In our experiments, N₂O₅ was alternately flowed over one of two aqueous solutions at the same

temperature but with differing chloride concentrations. The reference solution was saturated with NaCl (~6.1 M) while the chloride concentration of the sample solution was systematically varied. ClNO₂ formed from the reactive uptake of N₂O₅ to the chloride solutions was detected using chemical ionization mass spectrometry (CIMS) with a quadrupole mass analyzer and an ion source utilizing iodide anion cluster chemistry.³¹ We note that this experiment is unable to measure the absolute uptake of N₂O₅ into solution due to gas-phase diffusion limitations at atmospheric pressure; only product yields (and thus relative reaction rates for R1 and R2) can be determined. In the following sections we describe our experimental setup, the preparation of NaCl solutions, and our method for determining the ClNO₂ product yield.

Experimental Setup and Method. A schematic of the flow reactor and gas flow path is shown in Figure 1. The reactor consists of a milled aluminum block with PTFE solution holder inserts. The aluminum block contains coolant channels which enable thermal control via a recirculating chiller. The solution holders are each milled out of single pieces of PTFE and include a PTFE lid, embedded in the aluminum lid of the reactor. In combination with PFA tubing, these pieces ensure that the entire flow path is minimally reactive towards N₂O₅.

The solution holders each measure 130 mm \times 19 mm \times 25 mm and can hold a maximum solution volume of 27.5 mL. A 6.5 mm hole at either end of the solution holder enables the passage of gas through the headspace above the solution. For the 20 mL solutions used in this study, the total headspace volume above each solution was \sim 11 mL and the solution surface area was 14.5 cm².

As shown in Figure 1, dry N₂ is continually flowed over each solution at a rate of 1 liter per minute, while a computer-controlled solenoid valve controls the flow of the N₂O₅/NO₂/O₃/N₂ mixture into the system. This PTFE valve directs a 150 standard cubic centimeter per minute

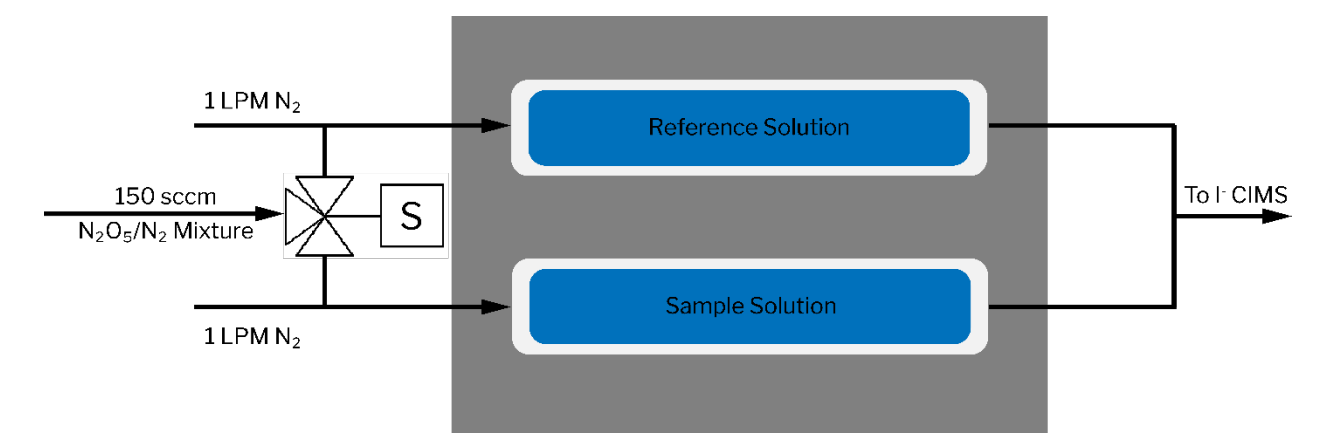


Figure 1. The flow path used in these experiments. The solenoid switching valve is computer controlled and all tubing is constructed of entirely inert materials.

(sccm) stream of N₂O₅ in N₂ into the carrier flow passing over either the sample or reference solution. Depending on the exact parameters of the N₂O₅ generation system, the concentration of N₂O₅ ranged from 100-150 ppb, but remained constant over the course of a single experiment. After passing over the solutions, the two carrier flows are recombined and sampled together by a chemical ionization mass spectrometer. We found it necessary to continuously maintain the carrier flow over each solution to prevent condensation on the dry walls of the solution holders, especially at lower temperatures.

The chemical ionization quadrupole mass spectrometer was operated in negative ion mode and utilized iodide cluster chemistry for the selective detection of ClNO₂ and N₂O₅ as the iodide adducts $I(ClNO_2)^-$ (m/Q of 207.87 Th) and $I(N_2O_5)^-$ (m/Q of 234.89 Th).³¹ These iodide adducts require the formation of $I(H_2O)_n^-$ clusters to form $I(ClNO_2)^-$ and $I(N_2O_5)^-$ via gas-phase ligand exchange reactions. We chose to use a weak electric field in the source region of the mass spectrometer to maximize the sensitivity to the iodide adduct analytes. However, this choice resulted in the efficient transmission of the $I(HNO_3 \cdot H_2O)^-$ (m/Q of 207.91 Th) cluster ion, which was not resolvable from $I(ClNO_2)^-$ (m/Q of 207.87 Th) by the quadrupole mass filter. To overcome

this overlap, we used D₂O in place of H₂O for the reference and sample solutions, which moved the $I(HNO_3 \cdot H_2O)^-$ peak to $I(DNO_3 \cdot D_2O)^-$ (m/Q of 210.92 Th). Tests described later indicate that the product yield increases slightly when substituting D₂O for H₂O.

It is well known that the sensitivity of iodide CIMS to various molecules can depend strongly on the absolute humidity within the ion molecule reactor.³² In our experiments the absolute humidity in the ion-molecule reaction region (IMR) is determined by D₂O evaporation from the sample and reference solutions. The symmetric nature of our experimental setup ensured that the absolute humidity in the IMR was independent of the flow path of N₂O₅ and remained constant over the course of an experiment. We tested this assumption by filling both the sample and reference solution holders with a saturated NaCl solution and monitored the I(N₂O₅)⁻ and I(ClNO₂)⁻ yields. In this configuration we observed a difference of less than 2% for ClNO₂, indicating that the sensitivity of the iodide CIMS was independent of the path taken by the N₂O₅.

Equipment Cleaning and Solution Preparation. To minimize the effects of any surfactant contaminants on our product yield measurements, all glassware and the PTFE solution holders were cleaned by immersion in concentrated H_2SO_4 for at least 30 minutes to dissolve residual surfactants and rinsed twice with ultrapure water to remove residual sulfate, which has also been shown to affect the ClNO₂ yield.¹³ Importantly, the addition of NaCl raised the surface tension of each solution, as expected in the absence of surfactants. Surface tension measurements of the 0.21, 0.54, and 2.4 M NaCl solutions yielded an average surface tension increment of 2.0 mN/m per molal in D_2O_2 , similar to the 1.7 \pm 0.2 mM/m per molal literature values in H_2O_2 . Following the sulfuric acid cleaning procedure, we prepared solutions of NaCl (EMD Millipore Corp. ACS Reagent Grade) in D_2O_2 (Sigma Aldrich, 99% D-atom) with concentrations of 0.0054,

0.014, 0.026, 0.055, 0.099, 0.21, 0.54, 2.4, and 6.1 M (saturated reference) in 25 mL volumetric flasks.

N₂O₅ Synthesis. N₂O₅ was generated in situ following the procedure described in Bertram et al.³⁴ Ultrapure zero air and ultrahigh purity nitrogen, each dried by passing the gas streams through potassium hydroxide traps, were mixed prior to illumination by a low-pressure mercury pen lamp (Jelight 95-2100-1), generating a stable concentration of ozone (O₃). The N₂/O₂/O₃ flow was then mixed with NO₂ delivered from a cylinder containing 50 ppm NO₂ in a balance of N₂. The gas mixture was subsequently mixed in a dark glass reaction cell for approximately 100 s. The resulting O₃, NO₂, NO₃, and N₂O₅ concentrations in the 150 sccm flow are estimated to be 360, 2700, 0.1, and 130 ppb, respectively, based on measurements of changes in the O₃ concentration as in Bertram et al.³⁴

Data Acquisition. In a typical experiment, each solution holder was filled with either a sample or reference solution and loaded into the reactor block. The reactor was then cooled to 5 °C with a recirculating chiller, and the temperature of the solutions was assumed to be equilibrated with the reactor block when the signals from the $I(D_2O)^-$ and $I(D_2O)_2^-$ cluster ions had stabilized. N_2O_5 was then passed over the NaCl solutions, with the flow alternating between the sample and reference solutions approximately every two minutes. To determine the ClNO2 production from the sample and reference solutions, the N_2O_5 flow was alternated at least 5 times for each temperature point. The temperature of the chiller was then increased and the signal intensities of the $I(D_2O)^-$ and $I(D_2O)_2^-$ cluster ions were monitored for temperature equilibration. Three experiments were performed for each NaCl sample concentration at temperatures of 5, 10, 15, 20, and 25 °C. Due to the larger range in ClNO2 product yields determined for the first three

experiments with the 2.4 M NaCl sample solution, a fourth experiment was performed only for this concentration.

Determination of Product Yield. The ClNO₂ product yield (Φ) is defined as the amount of ClNO₂ produced relative to the total amount of N₂O₅ lost by all reactions:

$$ClNO_2 \text{ Product Yield } (\Phi) = \frac{\Delta[ClNO_2]}{\Delta[N_2O_5]} = \frac{[ClNO_2]_{final}}{|[N_2O_5]_{initial} - [N_2O_5]_{final}|}$$
E1

where $\Delta[\text{CINO}_2]$ and $\Delta[\text{N}_2\text{O}_5]$ are the differences in the gas phase concentrations of CINO₂ and N₂O₅ before (initial) and after (final) exposure to the NaCl solution. Equation 1 assumes that there is no ClNO₂ in the incident gas stream. As in previous studies, we also assume that the ClNO₂ product yield from the saturated NaCl reference solution is 1 (i.e. all reacting N₂O₅ are converted into ClNO₂).^{13,35} This means that

$$\Phi \equiv 1 = \frac{\beta \, S_{\text{CINO}_2}(\text{Reference})}{\Delta [N_2 O_5](\text{Reference})}$$
 E2

and thus

$$\Delta[N_2O_5]$$
(Reference) = βS_{CINO_2} (Reference) E3

where S_{ClNO_2} is the ClNO₂ signal from the reference solution as measured by the mass spectrometer and β is the instrumental sensitivity factor. In the same way, $\Delta[ClNO_2] = \beta S_{ClNO_2}$. In our experiment, we assume that β is equivalent for the reference and sample conditions as the absolute humidity is the same. At atmospheric pressure, gas-phase diffusive transport of N₂O₅ to the liquid controls the loss rate of N₂O₅ to the solution and we are not sensitive to changes in the reactive uptake coefficient at the surface. As a result, we can assume that $\Delta[N_2O_5]$ over both the sample and reference solutions is identical. These assumptions lead to the equality

$$\Delta[N_2O_5]$$
(Reference) = $\Delta[N_2O_5]$ (Sample) E4

and the product yield expression

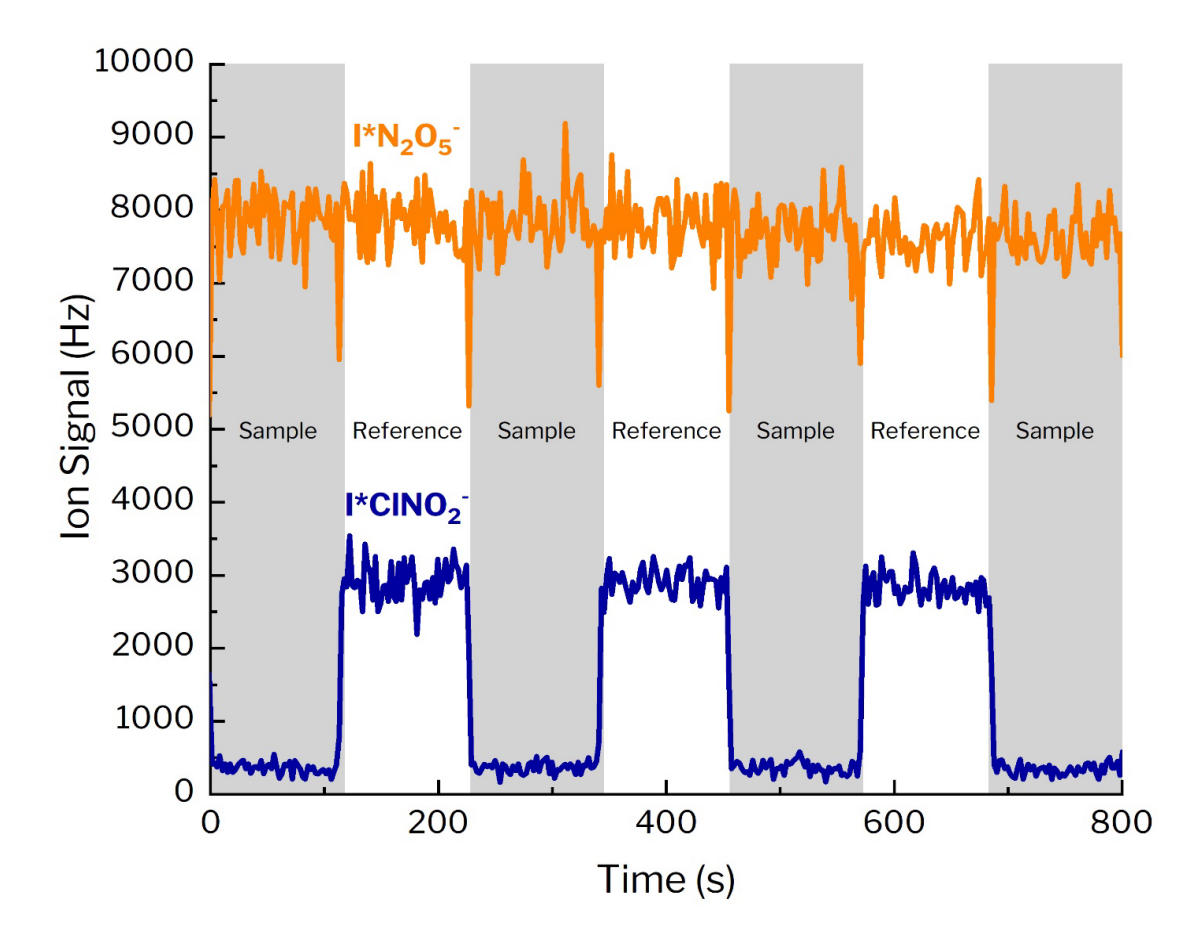


Figure 2. Representative experimental data showing the CIMS CINO₂ signal (S_{CINO2} , detected as $I(\text{CINO}_2)^-$, blue line) and the CIMS N_2O_5 signal (detected as $I(N_2O_5)^-$, orange line) when sampling from the flow reactor in the reference (non-shaded regions) and sample (shaded regions) solutions for sample [C_1^-] = 0.0054 M at 15 °C. The sharp dips in the N_2O_5 signal are due to the switching time of the solenoid valve and last no more than 1 s. Note the long-term stability of the N_2O_5 signal, which indicates both stable production of N_2O_5 during an experiment and equal loss between the sample and reference paths.

$$\Phi = \frac{\Delta[\text{ClNO}_2](\text{Sample})}{\Delta[\text{N}_2\text{O}_5](\text{Sample})} = \frac{\Delta[\text{ClNO}_2](\text{Sample})}{\Delta[\text{N}_2\text{O}_5](\text{Reference})} = \frac{S_{\text{ClNO}_2}(\text{Sample})}{S_{\text{ClNO}_2}(\text{Reference})}$$
 E5

This final expression states that the ClNO₂ product yield can simply be computed from the ratio of the ClNO₂ signals detected by the mass spectrometer from the sample and reference gas streams.

This method reduces the dependence of the retrieved ClNO₂ product yield on N₂O₅ loss in the transfer tubing that connects the reactor with the CIMS, which can be a significant fraction of the total N₂O₅ loss. Additionally, while the production rate of N₂O₅ on a given day was very stable, day-to-day variations of up to 50% were observed due to subtle changes in the gas flow rates used to generate the 150 sccm N₂O₅ stream. These day-to-day variations in incipient N₂O₅ concentrations resulted in variable ClNO₂ production from our aqueous solutions. We accounted for these variations by treating the saturated reference solution as an internal standard, thus removing the impact of gas phase N₂O₅ concentrations on our measurements. Also, embedded in our analysis are the assumptions that ClNO₂ is produced only over the solutions and that ClNO₂ does not undergo hydrolysis on the tubing walls. ^{13,36}

Data from a typical experiment is shown in Figure 2. As expected, the ClNO₂ yield is very responsive to the solution phase chloride concentration, with the reference solution producing more ClNO₂ than the 0.0054 M sample solution. An analysis of this data at different temperatures and NaCl concentrations is presented below.

RESULTS AND DISCUSSION

In this section we describe the results of our investigation, including the temperature dependent measurements of the $ClNO_2$ product yield and the effects of our use of D_2O solvent. We also carry out an Arrhenius analysis to determine the difference in activation energies between hydrolysis and chlorination and the ratio of pre-exponential factors for the two reactions.

Measurement of CINO₂ Product Yield. Figure 3 shows the CINO₂ product yield (Φ) calculated from eq 5 as a function of temperature from 5 to 25 °C for NaCl solutions between 0.0054 and 2.4 M. The product yield increases significantly with increasing Cl⁻ concentration, as expected from previous studies, ^{8,9,12,13,37} while the dependence on temperature is much less

apparent. Table 1 lists the average values of Φ at 5 and 25 °C, and data for all temperatures is included in the Supporting Information (SI). These results indicate that chloride concentration has a much larger impact on Φ than does temperature over the temperature and chloride concentrations used in this study.

Figure 3 shows that the ClNO₂ product yields decrease slightly with increasing temperature at lower Cl⁻ concentrations (≤ 0.21 M), while the 0.54 and 2.4 M solutions deviate from this behavior. Noticeably, the spread in the measured ClNO₂ product yield for these two higher concentration solutions increases significantly with increasing temperature. While collecting the data in Figure 3, it was necessary to replace the 50 ppm NO₂/N₂ cylinder and following this replacement it was noted the new measured concentration of DNO₃ was approximately 40% of the DNO₃ present with the original NO₂/N₂ cylinder. Interestingly, the measured ClNO₂ product yields for the 0.54 and 2.4 M solutions prior to the cylinder change (circles and squares in Figure 3) and those following the change (upward and downward triangles) exhibit different behaviors at higher temperatures. Due to the intricate interdependencies of the chemistries present within the ionmolecule reactor, ³⁸ we hypothesize that the decrease in DNO₃ afforded by the replacement NO₂/N₂ tank in combination with the increase in absolute humidity at higher temperatures resulted in a small differential sensitivity of the iodide CIMS to ClNO₂ for these solutions. This differential sensitivity resulted in large variations of the data obtained during different experiments, and for this reason we have removed the data from the 0.54 and 2.4 M solutions from our analysis.

Analysis of Competitive Hydrolysis and Chlorination. Beyond the importance of ClNO₂ formation in the atmosphere, the hydrolysis and chlorination reactions R1 and R2 represent a fundamentally interesting class of competitive reactions, in that one of the reacting molecules is

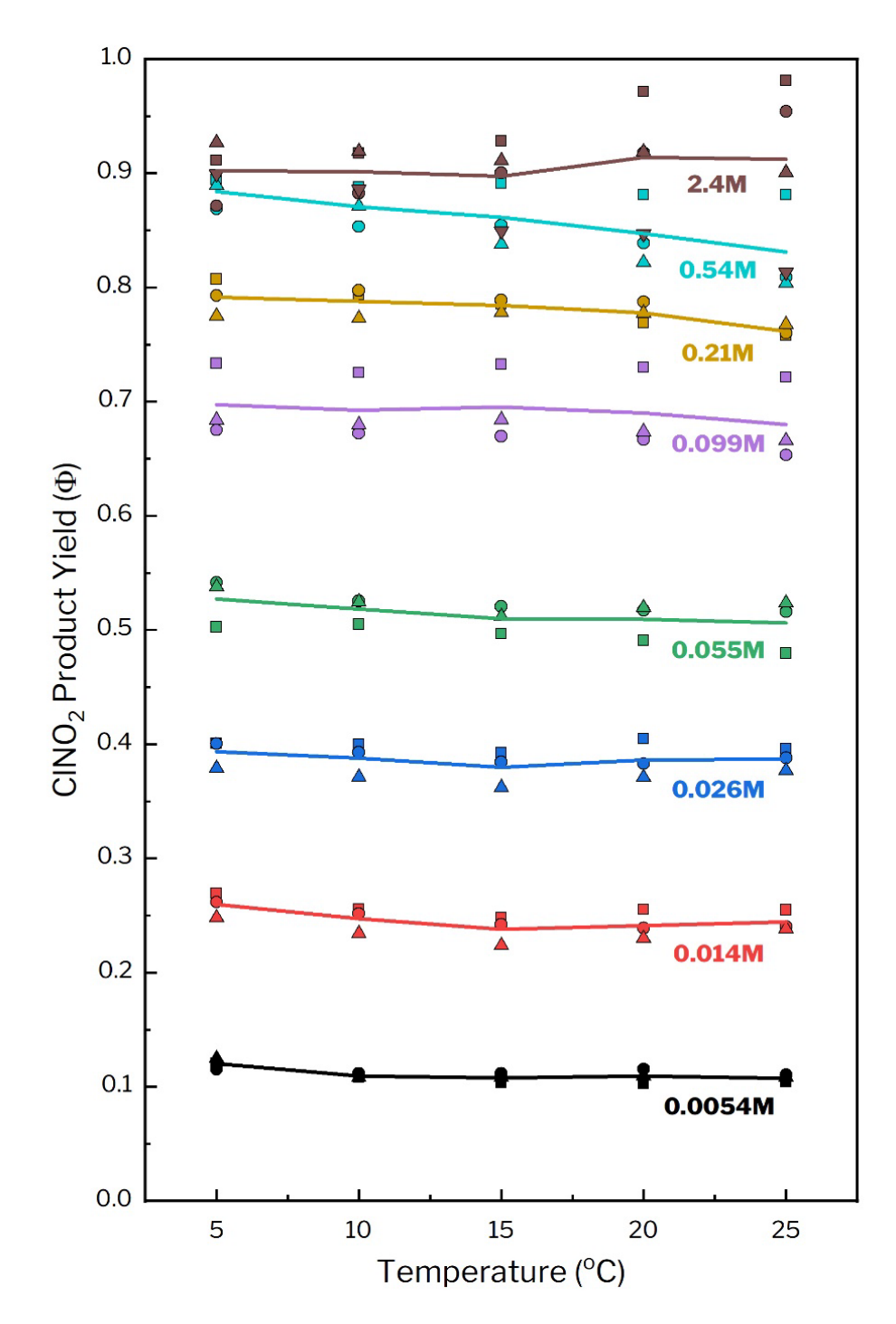


Figure 3. The product yield of ClNO₂ was measured for NaCl solutions in D₂O between 0.0054 M and 2.4 M and from 5 to 25 °C in 5-degree intervals. The different symbols represent the product yield calculated measured from each individual data acquisition run. Solid lines connect the means of the individual product yields for each NaCl concentration at each temperature point.

solvent water and the other is a solute chloride ion. We first consider whether hydrolysis and chlorination are under kinetic or thermodynamic control, based on experimental trends and the thermochemistry of each reaction:³⁹

$$\begin{split} N_2O_5(g) + H_2O &\to 2NO_3^- + 2H^+ \\ \Delta H^\circ = -142\frac{kJ}{mol} \ \Delta S^\circ = -134\frac{J}{mol\,K} \ \Delta G^\circ = -103\frac{kJ}{mol} \ K_{eq}(25\,^\circ\text{C}\,) = \ 1\times10^{18} \\ N_2O_5(g) + Cl^- &\to ClNO_2(g) + NO_3^- \\ \Delta H^\circ = -40\frac{kJ}{mol} \ \Delta S^\circ = +10\frac{J}{mol\,K} \ \Delta G^\circ = -43\frac{kJ}{mol} \ K_{eq}(\ 25\,^\circ\text{C}\,) = \ 3\times10^7 \end{split}$$

The ratio of equilibrium constants $K_{\rm eq}({\rm Cl}^-)/K_{\rm eq}({\rm H}_2{\rm O})$ is 3×10^{-11} at 25 °C, in contrast to the observed nearly complete conversion of N₂O₅ into ClNO₂ at only 2 M NaCl.⁸ The listed enthalpies and entropies also predict a significant temperature dependence, such that $K_{\rm eq}({\rm Cl}^-)/K_{\rm eq}({\rm H}_2{\rm O})$ increases by 17-fold upon cooling from 25 to 5 °C. Our ClNO₂ product yields below show a much weaker temperature dependence. The thermochemical data and experimental comparisons together imply that hydrolysis and chlorination generate products that are much more stable than the N₂O₅ reactant, and that the highly insoluble ClNO₂ rapidly evaporates from solution (with an estimated solubility of only ~0.04 M/atm at 25 °C⁴⁰), leading to nearly irreversible reactions for which N₂O₅ reactivity is controlled by the forward rates of R1 and R2.

We therefore consider the ClNO₂ product yield to be governed by the relative forward rates of N₂O₅ chlorination and hydrolysis as elementary reactions. The rate expressions can be written as $R_{\text{Chlorination}} = k_{\text{Cl}} - [\text{Cl}^-][\text{N}_2\text{O}_5]$ and $R_{\text{Hydrolysis}} = k_{\text{w}}[\text{D}_2\text{O}][\text{N}_2\text{O}_5]$ where k_{Cl} and k_{w} are the bimolecular rate constants for chlorination and hydrolysis. We can then express the ClNO₂ product yield for the sample solution as a quotient of reaction rates:

$$\Phi = \frac{\Delta[\text{ClNO}_2]}{\Delta[\text{ClNO}_2] + \Delta[\text{DNO}_3]} = \frac{R_{\text{Chlorination}}}{R_{\text{Chlorination}} + R_{\text{Hydrolysis}}} = \frac{k_{\text{Cl}} - [\text{Cl}^-][\text{N}_2\text{O}_5]}{k_{\text{Cl}} - [\text{Cl}^-][\text{N}_2\text{O}_5] + k_{\text{w}}[\text{D}_2\text{O}][\text{N}_2\text{O}_5]}}$$
(E6)

While we cannot independently determine k_{Cl} or k_{w} , we can compute their ratio by rearranging eq 6 to

$$\frac{k_{\text{Cl}^-}}{k_w} = \left(\frac{\Phi}{1-\Phi}\right) \frac{[D_2 O]}{[\text{Cl}^-]} \tag{E7}$$

Calculated values of $\frac{k_{Cl}}{k_w}$ are listed in Table 1 at 5 and 25 °C; the ratio $\frac{k_{Cl}}{k_w}$ shows little dependance on [Cl⁻] from 0.0054 to 0.21 M, typically decreasing by ~5% over the 20 °C range. At 25 °C, the average ratio $\frac{k_{\text{Cl}}}{k_{\text{Cl}}}$ from 0.0054 M to 0.21 M is 1139 ± 65, which is in line with the value of 836 ± 32 reported by Behnke et. al.⁸ but significantly larger than values of 483 ± 175 , 450 ± 100 , and 505 ± 190 reported of by Bertram and Thornton, Roberts et. al., 11 and Ryder et. al. 12 respectively. We note however that the smaller values were obtained from solutions or particles containing nitrate, bisulfate, or simulated seawater respectively, which have been shown to reduce the ClNO₂ product yield as compared with pure aqueous NaCl solutions. Table 1 also reveals that $\frac{k_{\text{Cl}}}{k_{\text{NL}}}$ (25) °C) declines steadily to 240:1 as the NaCl concentration increases from 0.1 to 2.4 M. This discrepancy is not improved by substituting NaCl and water activities for concentrations, which alter $\frac{k_{\text{Cl}}}{k_{\text{cr}}}$ by only a few percent in the opposite direction, suggesting that pre-existing interactions among Na+, Cl-, and water do not account for this drop.41 The large experimental uncertainties present in the [Cl⁻] \geq 0.54 M solutions make us hesitant to include the $\frac{k_{\text{Cl}}}{k_{\text{w}}}$ values for these higher concentration solutions when reporting a single rate constant ratio as has been done previously, and thus we have removed the values obtained with the 0.54 and 2.4 M solutions from the average values in Table 1. We note however that the downward trend with increasing [Cl⁻] may point to a

Table 1. ClNO₂ Product Yields and Rate Constant Ratios at 5 and 25 °C.^a

[Cl ⁻] (M)	Φ (5°C)	Φ (25°C)	$\frac{k_{\text{Cl}^-}}{k_{\text{w}}}(5^{\circ}C)$	$\frac{k_{\rm Cl}^-}{k_{\rm w}}(25^{\circ}C)$	$\frac{\frac{k_{\text{Cl}^-}}{k_{\text{w}}}(5^{\circ}C)}{\frac{k_{\text{Cl}^-}}{k_{\text{w}}}(25^{\circ}C)}$
0.0054	0.120 ± 0.008	0.108 ± 0.006	1391 ± 50	1222 ± 35	1.14 ± 0.04
0.014	0.260 ± 0.018	0.245 ± 0.015	1378 ± 63	1249 ± 51	1.08 ± 0.06
0.026	0.393 ± 0.021	0.387 ± 0.016	1372 ± 59	1341 ± 44	1.02 ± 0.05
0.055	0.527 ± 0.036	0.506 ± 0.040	1115 ± 79	1018 ± 79	1.10 ± 0.10
0.099	0.697 ± 0.053	0.680 ± 0.061	1280 ± 160	1170 ± 160	1.10 ± 0.17
0.21	0.791 ± 0.027	0.762 ± 0.009	995 ± 80	833 ± 19	1.19 ± 0.07
0.54	0.884 ± 0.023	0.831 ± 0.073	782 ± 78	500 ± 131	1.56 ± 0.18
2.4	0.902 ± 0.028	0.912 ± 0.087	214 ± 51	239 ± 411	0.89 ± 1.96
Average ^b	$\langle \Phi(5 ^{\circ}\text{C})/\Phi(25 ^{\circ}\text{C}) \rangle = 1.047 \pm 0.026$		1255 ± 81	1139 ± 65	1.10 ± 0.08

 $^{^{\}rm a}$ The error bars in Φ are equal to 90% confidence intervals for the 3 (or 4) measurements at each temperature.

rate constant ratio for chlorination and hydrolysis that depends on interactions between Cl⁻ and N₂O₅ not taken into account in the rate expressions in Eq 6.

Impacts of Using D₂O. Figure 4 compares the ClNO₂ product yields obtained in our study with values obtained by previous investigators at room temperature. 8,9,11,12 Notably, our measured product yields are larger than those previously reported. In addition to the added ion effect present in many of the previous experiments, such as the inclusion of sulfate and nitrate, we were curious if our use of D₂O solvent instead of H₂O impacted our measurements. This effect can be investigated by slightly modifying the experiment to measure the ClNO₂ product yield in H₂O. The sample solution holder was filled with a solution of 0.097 M NaCl in H₂O and the reference solution holder with a saturated NaCl solution in H₂O. Due to the interference in the mass spectrometer of I(HNO₃·H₂O)⁻ detected at m/Q of 207.91 Th with I(ClNO₂)⁻ detected at m/Q of

^b Due to the large experimental uncertainty, the data from the 0.54 and 2.4 M solutions is excluded from the calculation of the average.

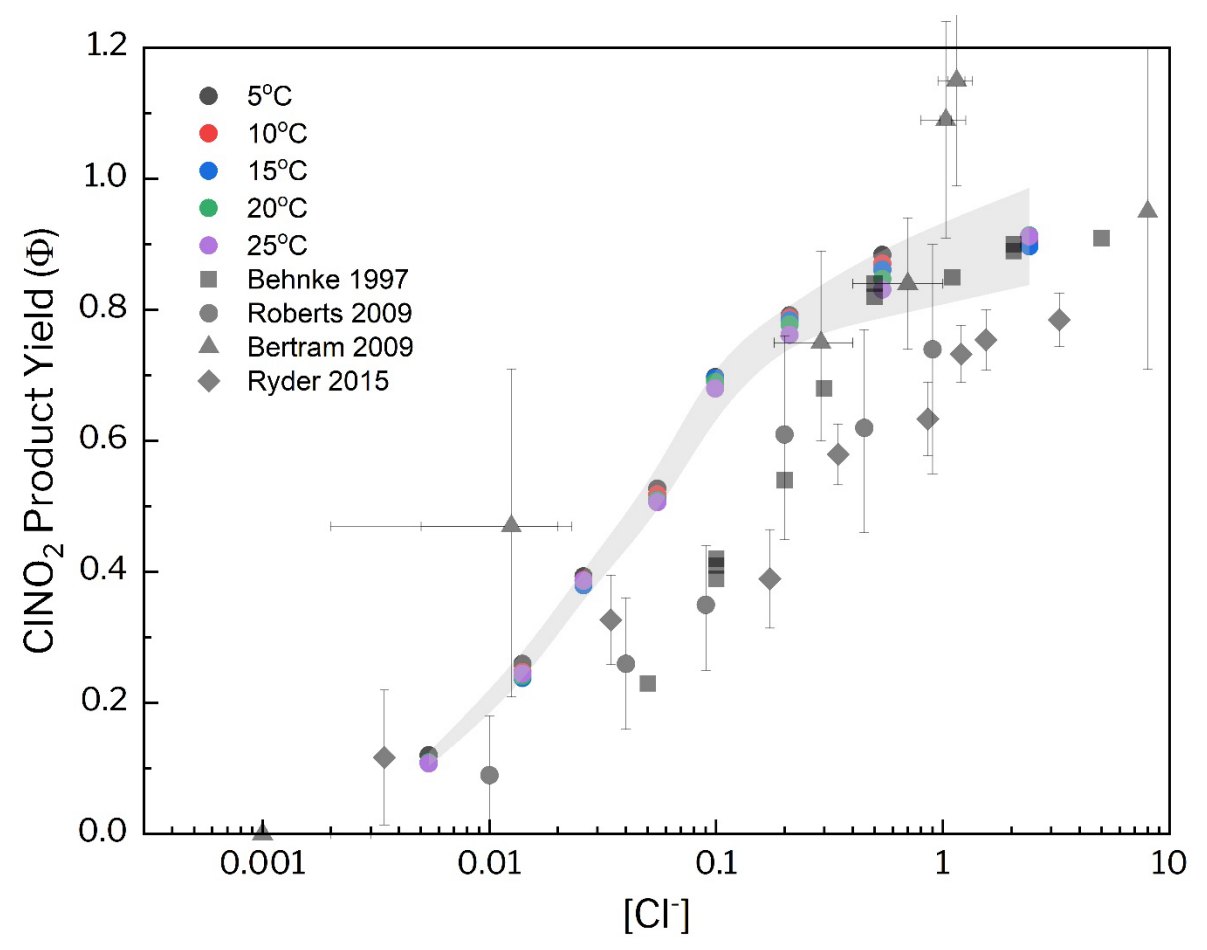


Figure 4. Values of the ClNO₂ Product Yield as a function of chloride concentration from this study superimposed onto data from previous laboratory experiments. At each concentration, the grey band indicates ±1 standard deviation as determined by the temperature measurement with the largest standard deviation.

207.87 Th, we introduced supplemental D₂O vapor into the transfer line between the flow reactor and the mass spectrometer and cooled the flow reactor to 5 °C to reduce H₂O evaporation. This experiment could only be conducted at 5 °C where enough D₂O could be added to the ion molecule reaction region to suppress I(H₂O)⁻ chemistry. At higher solution temperatures, and thus H₂O vapor pressures, I(H₂O)⁻ remained the dominant reagent ion. We performed the H₂O experiments twice

at 0.097 M NaCl in H₂O and obtained product yields of 0.63 and 0.62. These values are 11-12% lower than the product yields of 0.70 observed from our D₂O solution at a nearly identical concentration of 0.099 M NaCl. Using eq 7, we calculate $\frac{k_{Cl}}{k_{w}}$ to be approximately 1.4 times larger in H₂O than in D₂O, which is within the range of reported values for the kinetic isotope effect in the H₂O/D₂O system.⁴² This isotope effect may arise in part from the slower motions of D₂O molecules and their weaker autoionization. When we correct our average value for this effect we find a value of k_{Cl} – $/k_{w}$ (H₂O, 5°C) = 896 ± 58, remarkably close to the value of 836 ± 32 reported by Behnke at room temperature.⁸

Arrhenius Analysis. We next carry out an Arrhenius analysis of R1 and R2 to determine the difference in activation energies between chlorination and hydrolysis, along with the ratio of pre-exponential factors. The Arrhenius expressions for the rate constants in R1 and R2 are $k_{\text{Cl}^-} = A_{\text{Cl}^-} e^{-E_{\text{Cl}^-}}/RT$ and $k_w = A_{\text{w}} e^{-E_{\text{w}}}/RT$, where A_{Cl^-} and A_{w} are the respective pre-exponential factors for chlorination and hydrolysis and E_{Cl^-} and E_{w} are the activation energies. These expressions enable us to rewrite the ClNO₂ product yield (eq 6) as

$$\Phi = \frac{1}{1 + \frac{A_{\text{Cl}} - [\text{Cl}^{-}]}{A_{\text{W}}[\text{D}_{2}\text{O}]} e^{\frac{-\Delta E}{RT}}}$$
(E8)

where $\Delta E = E_{\text{Cl}} - E_{\text{w}}$ is the difference in activation energies between chlorination and hydrolysis. To determine ΔE and the ratio of pre-exponential factors from the data, we rearrange eq 8 into a linear form

$$\ln\left(\frac{\Phi}{1-\Phi}\right) = -\frac{\Delta E}{R} \frac{1}{T} + \ln\left(\frac{A_{\text{Cl}} - [\text{Cl}]}{A_{\text{W}}[D_2O]}\right)$$
 (E9)

A plot of the product yield data in the form of eq 9 is shown in Figure 5A, with a magnified view of the data for the 0.055 M solution shown in Figure 5B. The slopes of these lines are proportional

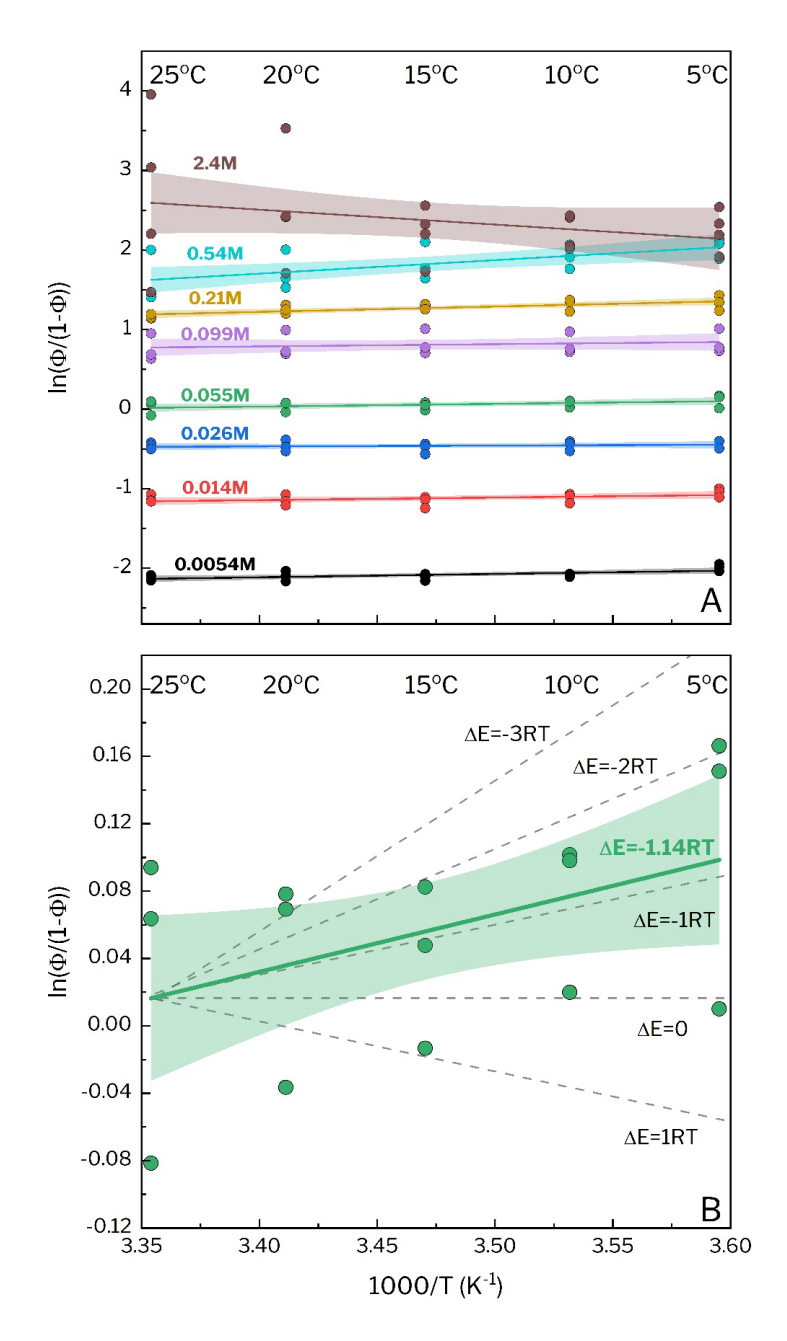


Figure 5. A) ClNO₂ product yield Φ plotted in the form of Eq 9. Note the similar slope of all solutions with [Cl⁻] \leq 0.21 M. B) Expanded view of the data for 0.055 M NaCl showing the linear fit. The shaded dashed lines have slopes corresponding to integer multiples of RT for comparison. In both panels, the shaded region represents the 90% confidence interval for the line of best fit.

to $-\Delta E/R$ for the competing reactions, while the y-intercept is equal to $\ln\left(\frac{A_{\rm Cl}^{-}[{\rm Cl}^{-}]}{A_{\rm w}[{\rm D}_2{\rm O}]}\right)$ based on a linear extrapolation. The data for each solution are offset due to the [Cl-] dependance of the y-intercept. As seen in panel A, the plots of the low concentration data have very similar positive slopes, corresponding to small negative ΔE values. Panel B reflects the scatter in the data with respect to slopes in units of RT. The extracted ΔE values and $A_{\rm Cl}^{-}/A_{\rm w}$ ratios are listed in Table 2. We note that the large spread in the $\ln\left(\frac{\Phi}{1-\Phi}\right)$ values obtained from the 0.54 and 2.4 M solutions results in large uncertainties when fitting the slope and intercept, and we have removed these data sets from the average values listed at the bottom of the table.

The resulting average ΔE value of -3.0 \pm 1.8 kJ/mol indicates that the energetic barrier to chlorination is slightly less than to hydrolysis; at 25 °C this difference in activation energies corresponds to only 1.2 RT and a Boltzmann factor of $e^{-\Delta E/RT} = 3.4$. This surprisingly small factor is a key conclusion of our study: Cl⁻ and D₂O attack on N₂O₅ have similar energetic barriers despite the differences in charge and complexity of the Cl⁻ and D₂O reactants. As the measured rate constant for chlorination is approximately one thousand times larger than for hydrolysis, the difference in rate constants must be driven by the pre-exponential ratio, and indeed we extract an average A_{Cl^-}/A_w to be 419⁺⁵⁴²₋₂₁₅ at 25 °C.

There are currently no measurements of the individual activation energies for hydrolysis or chlorination and theoretical studies have been limited. Work by Gerber and coworkers locate a barrier of 50 kJ/mol for N₂O₅(H₂O)₂₀ for hydrolysis and 31 kJ/mol for chlorination in a [ClN₂O₅(H₂O)₁₂] cluster^{10,25} These calculations qualitatively agree with our experimental finding that chlorination is more favorable than hydrolysis, though the calculated difference of 19 kJ/mol is larger than the 3 kJ/mol value we have obtained. Generally, such computational studies indicate that hydrolysis proceeds from a hydrophobically solvated N₂O₅ molecule with weak hydrogen

Table 2. Calculated Values of ΔE and $A_{\text{Cl}^-}/A_{\text{w}}$ for the solutions measured in this study. Due to the large experimental uncertainty as seen in Figure 5A, the data from the 0.54 and 2.4 M solutions is excluded from the average.

[Cl ⁻] (M)	ΔE (kJ/mol)	$\frac{A_{Cl}^-}{A_w}$	
0.0054	-3.5 ± 1.3	292+202	
0.014	-2.7 ± 1.6	414^{+386}_{-200}	
0.026	-0.88 ± 1.4	925^{+731}_{-408}	
0.055	-2.8 ± 1.6	324^{+303}_{-157}	
0.099	-2.3 ± 3.5	471 ⁺¹⁵⁵²	
0.211	-5.6 ± 1.5	90 ⁺⁷⁹ ₋₄₂	
0.54	-14.1 ± 5.1	$1.8^{+12.9}_{-1.6}$	
2.4	15.5 ± 12.6	$1.63x10^{5^{+3.17}x10^{7}}_{-1.62x10^{5}}$	
Average	-3.0 ± 1.8	419 ⁺⁵⁴² ₋₂₁₅	

bonding but significant and fluctuating ion-pair character, $NO_2^{\delta+}NO_3^{\delta-}.^{25-27}$ Hydrolysis can proceed by nucleophilic attack of $OH^{\delta-}$ on $NO_2^{\delta+}$ or electrophilic attack of $H^{\delta+}$ on $NO_3^{\delta-}$. In both cases, solvent water molecules may rearrange into more structured configurations to stabilize a transition state consisting of ion pair-like $NO_2^{\delta+}NO_3^{\delta-}$ and adjacent $H^{\delta+}OH^{\delta-}$. In contrast, attack of CI^- on $NO_2^{\delta+}NO_3^{\delta-}$ may involve the transformation of tightly bound water molecules around the CI^- ion into a looser structure around a larger and more charge diffuse $[CIN_2O_5]^-$ transition state. The enthalpic penalty incurred upon de-solvation of the CI^- ion may be partially compensated by an entropic benefit resulting from the co-solvation of CI^- and N_2O_5 within the same solvent pocket, while CI^- itself may assist in inducing charge separation in N_2O_5 and thus facilitate chlorination.

Using the measured ratio of rate constants and solute and solvent standard states $c^{\circ}(\text{Cl}^{-}) = 1 \text{ M}$ and $c^{\circ}(\text{D}_{2}\text{O}) = 55.1 \text{ M}$, we compute a difference in free energy barriers of $\Delta \Delta F^{\ddagger} = -RT \ln \left(\frac{k_{\text{Cl}} - c^{\circ}(\text{Cl}^{-})}{k_{\text{W}} c^{\circ}(\text{D}_{2}\text{O})} \right) = -7 \pm 2 \text{ kJ/mol}$, about twice the value measured from the change in

activation energy. This remaining difference comes from the pre-exponential factor that in principle includes both dynamic and entropic contributions to the relative rates. Entropic contributions are fundamentally molecular and can be explored with simulation techniques. While a full understanding of the molecular underpinnings of the relative driving forces for hydrolysis

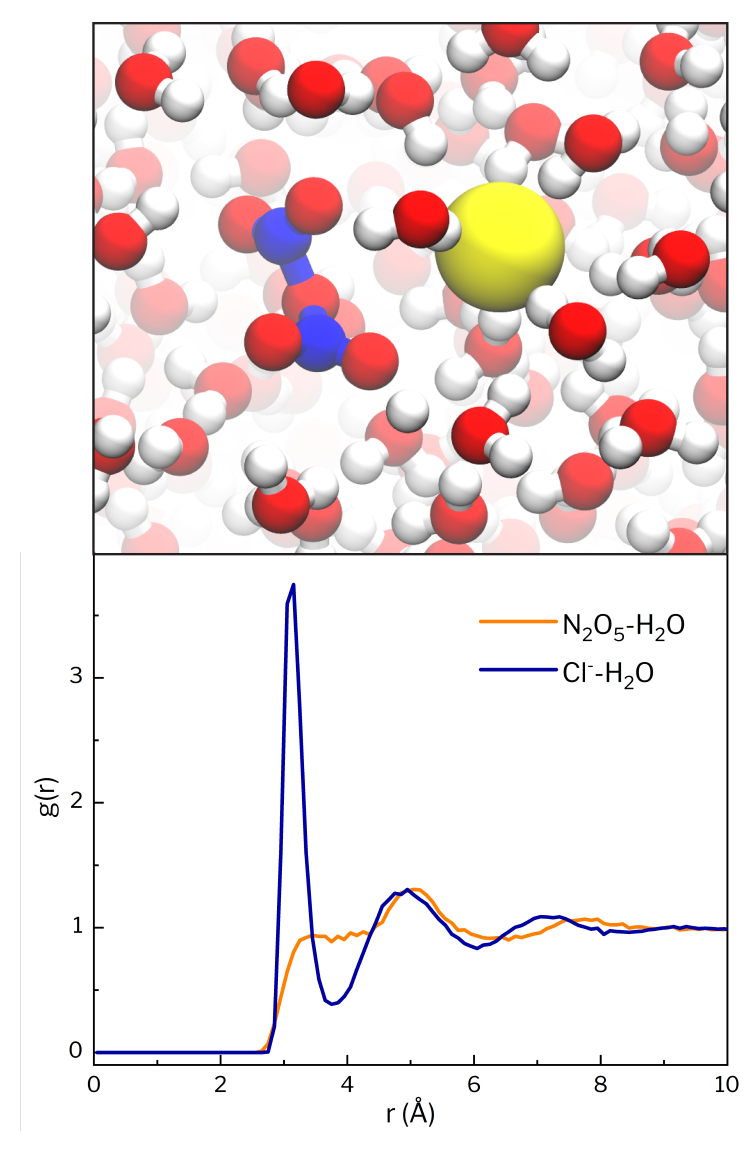


Figure 6. Characteristic snapshot of the solvated N_2O_5 and Cl^- complex (top) and the radial distribution functions between the solute centers and surround water (bottom). See the Supporting Information for a description of the theoretical methods.

and chlorination is beyond the scope of the current work, the results of molecular dynamics simulations employing optimized point charge models of N_2O_5 and Cl^- shown in Figure 6 illustrate a dramatic difference between their local solvation environments. Shown are the radial distribution functions, g(r), between the water and each solute, where the hydrophobic solvation of N_2O_5 is evident by its unstructured density profile, while the highly hydrophilic solvation of Cl^- is clear by the prominent first solvation shell structure. A potential entropic difference between hydrolysis and chlorination may thus arise from solvent water rearrangements as reactants evolve into their transition states. Such studies are on-going.

Apart from entropic contributions, the relative pre-exponential factors to the rates of chlorination and hydrolysis encode fundamentally dynamical information. The dynamic contribution to the rate ratio reflects differences in the flux of reactants over the relevant transition states, which consist of contributions from both diffusive fluxes for the two species to meet each other in space and attempt frequencies to overcome the reaction barriers. While there is not a direct measurement of either the absolute chlorination or hydrolysis rates, recent theoretical work combining molecular simulation and observed gaseous uptake measurements has narrowed a likely value of the hydrolysis rate constant in pure water to be $k_w = 7 \times 10^5 / \text{M/s}.^{27}$ Because this simulation neglects nuclear quantum effects, it should be more applicable to the D₂O solutions investigated here than to H₂O solutions. Taking the branching ratio of 1139 from our 25 °C low concentration measurements (averaged between 0.0054 and 0.21 M), the chlorination rate constant is estimated to be $k_{\text{Cl}^-} = 8 \times 10^8 / \text{M/s}.$

To understand potential dynamical effects, we can estimate the rate of chlorination assuming it proceeds in the diffusion limit. Under dilute solution conditions, the diffusion constants for N_2O_5 and Cl^- are approximately $D_{N2O5} = 1.6 \times 10^{-5} \text{cm}^2/\text{s}$ and $D_{Cl}^- =$

 1.7×10^{-5} cm²/s at 25 °C (scaled from their values in H₂O to D₂O by multiplying by 0.82.)^{27,43} Assuming a capture radius of $\lambda = 3.1$ Å, taken from the peak in the first solvation shell of the two solutes in Figure 6, the diffusion-limited rate constant can be estimated as $k_{\text{Cl}}^{\text{diff}} = 4\pi (D_{\text{N2O5}} + D_{\text{Cl}})\lambda = 8 \times 10^9 / \text{M/s}$, roughly an order of magnitude faster than the estimated rate constant. This calculation is both temperature and concentration dependent: at 5 °C the Cl diffusion constant is 58% of the value at 25 °C, while in a 2.4 M NaCl solution the Cl diffusion constant is 77% of the infinite dilution value.⁴⁴ Together, these estimates suggest that the temperature and salt concentration dependence of the diffusion coefficients themselves may explain part of the trends in Table 1. We are currently investigating the mechanism for chlorination in extended water simulations, 10,29,30 which when compared with the mechanism for hydrolysis, 23,24 will hopefully explain the small difference in activation energies and large difference in activation entropies between these ion-neutral solute-solute and neutral-neutral solute-solvent reactions.

SUMMARY AND CONCLUSIONS

We have measured the temperature dependence of the ClNO₂ product yield over 5 to 25 °C following N₂O₅ reactive uptake to 0.0054 to 2.4 M NaCl/D₂O solutions. The ClNO₂ yield decreases on average by less than 5% over this 20 °C range, with less reproducible results at 0.54 and 2.4 M NaCl. An Arrhenius analysis leads to a difference in activation energies between chlorination and hydrolysis, $E_{\text{Cl}^-} - E_{\text{w}}$, of only -3.0 ± 1.8 kJ/mol (on par with thermal energy at room temperature), despite a thousand-fold greater rate constant for chlorination than for hydrolysis. These two measurements in turn reflect a ratio of Arrhenius pre-exponential factors, $\left(\frac{A_{\text{Cl}^-}}{A_{\text{w}}}\right)$, equal on average to 419^{+542}_{-215} . This large ratio implies that the difference in rate constants is primarily driven by dynamic and entropic rather than enthalpic considerations, perhaps due to

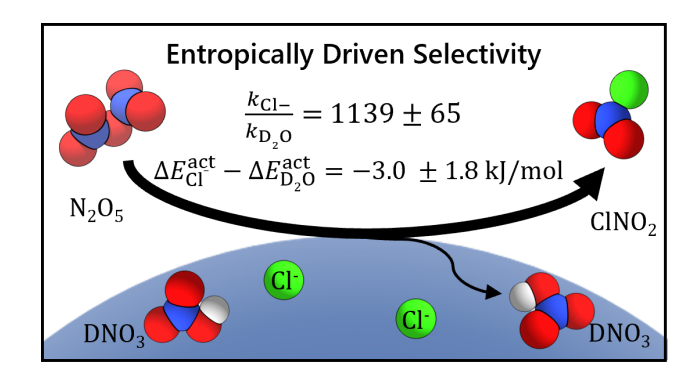
different solvent shell rearrangements required to stabilize the respective transition states. We are now exploring the mechanisms for chlorination and hydrolysis by machine learning reactive many body potentials to understand the origins of these entropic effects.²⁶

The small change in ClNO₂ product yield over 5 to 25 °C suggests that its temperature dependence will not play a large role in atmospheric models in this temperature range. However, these results have been obtained only for pure sodium chloride solutions. As shown previously, the addition of sulfate or acetate ions, the neutral surfactant phenol, or humic acid each significantly reduces the production of ClNO₂ from N₂O₅ reactive uptake, in all cases by more than two fold.^{12,13} These ions and organic surfactants are ubiquitous components of sea spray.⁴⁵ Recent ab initio molecular dynamics calculations further indicate that S_N2 reactions of sulfate and formate leading to hydrolysis of N₂O₅ proceed with barriers that are 17 and 13 kJ/mol lower, respectively, than reactions with chloride leading to ClNO₂.¹⁰ These calculations imply that sulfate and carboxylate anions may compete even more favorably at lower temperatures, and thereby reduce the ClNO₂ yield beyond chloride alone, potentially leading atmospheric models to overestimate its abundance. Experiments testing this hypothesis will help unravel multiple competitive hydrolysis and halogenation reactions occurring in sea spray aerosols over a range of temperatures and compositions.

ACKNOWLEDGMENTS

This work was funded by the National Science Foundation through the National Science Foundation Center for Aerosol Impacts on Chemistry of the Environment (NSF-CAICE) under Grant No. CHE 1801971. We thank R. Benny Gerber, Natalia Karimova, Andreas Götz, and Mark Johnson for many enlightening discussions.

Table of Contents graphic



REFERENCES

- (1) Chang, W. L.; Brown, S. S.; Stutz, J.; Middlebrook, A. M.; Bahreini, R.; Wagner, N. L.; Dubé, W. P.; Pollack, I. B.; Ryerson, T. B.; Riemer, N. Evaluating N₂O₅ Heterogeneous Hydrolysis Parameterizations for CalNex 2010. *J. Geophys. Res. Atmos.* **2016**, *121* (9), 5051–5070. https://doi.org/10.1002/2015JD024737.
- (2) Brown, S. S.; Stutz, J. Nighttime Radical Observations and Chemistry. *Chem. Soc. Rev.* 2012, 41 (19), 6405–6447. https://doi.org/10.1039/C2CS35181A.
- (3) Simpson, W. R.; Brown, S. S.; Saiz-Lopez, A.; Thornton, J. A.; von Glasow, R. Tropospheric Halogen Chemistry: Sources, Cycling, and Impacts. *Chem. Rev.* **2015**, *115* (10), 4035–4062. https://doi.org/10.1021/cr5006638.
- (4) Sarwar, G.; Simon, H.; Xing, J.; Mathur, R. Importance of Tropospheric ClNO₂ Chemistry across the Northern Hemisphere. *Geophys. Res. Lett.* **2014**, *41* (11), 4050–4058. https://doi.org/10.1002/2014GL059962.
- (5) Macintyre, H. L.; Evans, M. J. Sensitivity of a Global Model to the Uptake of N₂O₅ by Tropospheric Aerosol. *Atmos. Chem. Phys.* **2010**, *10* (15), 7409–7414. https://doi.org/10.5194/acp-10-7409-2010.
- (6) Riemer, N.; Vogel, H.; Vogel, B.; Schell, B.; Ackermann, I.; Kessler, C.; Hass, H. Impact of the Heterogeneous Hydrolysis of N₂O₅ on Chemistry and Nitrate Aerosol Formation in the Lower Troposphere under Photosmog Conditions. *J. Geophys. Res. Atmos.* 2003, 108 (D4). https://doi.org/10.1029/2002JD002436.
- (7) Pathak, R. K.; Wang, T.; Wu, W. S. Nighttime Enhancement of PM2.5 Nitrate in Ammonia-Poor Atmospheric Conditions in Beijing and Shanghai: Plausible Contributions of

- Heterogeneous Hydrolysis of N₂O₅ and HNO₃ Partitioning. *Atmospheric Environ.* **2011**, *45* (5), 1183–1191. https://doi.org/10.1016/j.atmosenv.2010.09.003.
- (8) Behnke, W.; George, C.; Scheer, V.; Zetzsch, C. Production and Decay of ClNO₂ from the Reaction of Gaseous N₂O₅ with NaCl Solution: Bulk and Aerosol Experiments. *J. Geophys.* Res. Atmos. 1997, 102 (D3), 3795–3804. https://doi.org/10.1029/96JD03057.
- (9) Bertram, T. H.; Thornton, J. A. Toward a General Parameterization of N₂O₅ Reactivity on Aqueous Particles: The Competing Effects of Particle Liquid Water, Nitrate and Chloride. Atmospheric Chem. Phys. 2009, 9 (21), 8351–8363. https://doi.org/10.5194/acp-9-8351-2009.
- (10) Karimova, N. V.; Chen, J.; Gord, J. R.; Staudt, S.; Bertram, T. H.; Nathanson, G. M.; Gerber, R. B. S_N2 Reactions of N₂O₅ with Ions in Water: Microscopic Mechanisms, Intermediates, and Products. *J. Phys. Chem. A* 2020, 124 (4), 711–720. https://doi.org/10.1021/acs.jpca.9b09095.
- (11) Roberts, J. M.; Osthoff, H. D.; Brown, S. S.; Ravishankara, A. R.; Coffman, D.; Quinn, P.; Bates, T. Laboratory Studies of Products of N₂O₅ Uptake on Cl⁻ Containing Substrates. *Geophys. Res. Lett.* **2009**, *36* (20). https://doi.org/10.1029/2009GL040448.
- (12) Ryder, O. S.; Campbell, N. R.; Shaloski, M.; Al-Mashat, H.; Nathanson, G. M.; Bertram, T. H. Role of Organics in Regulating ClNO₂ Production at the Air–Sea Interface. *J. Phys. Chem.*A 2015, 119 (31), 8519–8526. https://doi.org/10.1021/jp5129673.
- (13) Staudt, S.; Gord, J. R.; Karimova, N. V.; McDuffie, E. E.; Brown, S. S.; Gerber, R. B.; Nathanson, G. M.; Bertram, T. H. Sulfate and Carboxylate Suppress the Formation of ClNO₂ at Atmospheric Interfaces. *ACS Earth Space Chem.* **2019**, *3* (9), 1987–1997. https://doi.org/10.1021/acsearthspacechem.9b00177.

- (14) Zhao, X.; Nathanson, G. M.; Andersson, G. G. Competing Segregation of Br⁻ and Cl⁻ to a Surface Coated with a Cationic Surfactant: Direct Measurements of Ion and Solvent Depth Profiles. *J. Phys. Chem. A* **2020**, *124* (52), 11102–11110. https://doi.org/10.1021/acs.jpca.0c08859.
- (15) McDuffie, E. E.; Fibiger, D. L.; Dubé, W. P.; Lopez Hilfiker, F.; Lee, B. H.; Jaeglé, L.; Guo, H.; Weber, R. J.; Reeves, J. M.; Weinheimer, A. J.; Schroder, J. C.; Campuzano-Jost, P.; Jimenez, J. L.; Dibb, J. E.; Veres, P.; Ebben, C.; Sparks, T. L.; Wooldridge, P. J.; Cohen, R. C.; Campos, T.; Hall, S. R.; Ullmann, K.; Roberts, J. M.; Thornton, J. A.; Brown, S. S. ClNO₂ Yields From Aircraft Measurements During the 2015 WINTER Campaign and Critical Evaluation of the Current Parameterization. *J. Geophys. Res. Atmos.* 2018, 123 (22), 12,994-13,015. https://doi.org/10.1029/2018JD029358.
- (16) Schweitzer, F.; Mirabel, P.; George, C. Multiphase Chemistry of N₂O₅, ClNO₂, and BrNO₂.
 J. Phys. Chem. A 1998, 102 (22), 3942–3952. https://doi.org/10.1021/jp980748s.
- (17) Gaston, C. J.; Thornton, J. A. Reacto-Diffusive Length of N₂O₅ in Aqueous Sulfate- and Chloride-Containing Aerosol Particles. *J. Phys. Chem. A* **2016**, *120* (7), 1039–1045. https://doi.org/10.1021/acs.jpca.5b11914.
- (18) Thornton, J. A.; Braban, C. F.; Abbatt, J. P. D. N₂O₅ Hydrolysis on Sub-Micron Organic Aerosols: The Effect of Relative Humidity, Particle Phase, and Particle Size. *Phys. Chem. Chem. Phys.* **2003**, *5* (20), 4593–4603. https://doi.org/10.1039/B307498F.
- (19) McNeill, V. F.; Patterson, J.; Wolfe, G. M.; Thornton, J. A. The Effect of Varying Levels of Surfactant on the Reactive Uptake of N₂O₅ to Aqueous Aerosol. *Atmospheric Chem. Phys.* 2006, 6 (6), 1635–1644. https://doi.org/10.5194/acp-6-1635-2006.

- (20) Stewart, D. J.; Griffiths, P. T.; Cox, R. A. Reactive Uptake Coefficients for Heterogeneous Reaction of N₂O₅ with Submicron Aerosols of NaCl and Natural Sea Salt. *Atmospheric Chem. Phys.* **2004**, *4* (5), 1381–1388. https://doi.org/10.5194/acp-4-1381-2004.
- (21) George, C.; Ponche, J. L.; Mirabel, P.; Behnke, W.; Scheer, V.; Zetzsch, C. Study of the Uptake of N₂O₅ by Water and NaCl Solutions. *J. Phys. Chem.* **1994**, *98* (35), 8780–8784. https://doi.org/10.1021/j100086a031.
- (22) Mozurkewich, M.; Calvert, J. G. Reaction Probability of N₂O₅ on Aqueous Aerosols. *J. Geophys. Res. Atmos.* **1988**, 93 (D12), 15889–15896. https://doi.org/10.1029/JD093iD12p15889.
- (23) Bianco, R.; Hynes, J. T. Theoretical Studies of Heterogeneous Reaction Mechanisms Relevant for Stratospheric Ozone Depletion. *Int. J. Quantum Chem.* **1999**, *75* (4–5), 683–692. https://doi.org/10.1002/(SICI)1097-461X(1999)75:4/5<683::AID-QUA35>3.0.CO;2-F.
- (24) McNamara, J. P.; Hillier, I. H. Structure and Reactivity of Dinitrogen Pentoxide in Small Water Clusters Studied by Electronic Structure Calculations. J. Phys. Chem. A 2000, 104 (22), 5307–5319. https://doi.org/10.1021/jp9942791.
- (25) Rossich Molina, E.; Gerber, R. B. Microscopic Mechanisms of N₂O₅ Hydrolysis on the Surface of Water Droplets. *J. Phys. Chem. A* **2020**, *124* (1), 224–228. https://doi.org/10.1021/acs.jpca.9b08900.
- (26) Galib Mirza; Limmer David T. Reactive Uptake of N2O5 by Atmospheric Aerosol Is Dominated by Interfacial Processes. *Science* **2021**, *371* (6532), 921–925. https://doi.org/10.1126/science.abd7716.

- (27) Cruzeiro, V. W. D.; Galib, M.; Limmer, D. T.; Götz, A. W. Uptake of N₂O₅ by Aqueous Aerosol Unveiled Using Chemically Accurate Many-Body Potentials. *Nat. Commun.* **2022**, *13* (1), 1266. https://doi.org/10.1038/s41467-022-28697-8.
- (28) Hirshberg, B.; Molina, E. R.; Götz, A. W.; Hammerich, A. D.; Nathanson, G. M.; Bertram, T. H.; Johnson, M. A.; Gerber, R. B. N₂O₅ at Water Surfaces: Binding Forces, Charge Separation, Energy Accommodation and Atmospheric Implications. *Phys. Chem. Chem. Phys.* 2018, 20 (26), 17961–17976. https://doi.org/10.1039/C8CP03022G.
- (29) McNamara, J. P.; Hillier, I. H. Exploration of the Atmospheric Reactivity of N₂O₅ and HCl in Small Water Clusters Using Electronic Structure Methods. *Phys. Chem. Chem. Phys.* 2000, 2 (11), 2503–2509. https://doi.org/10.1039/B001497O.
- (30) Hammerich, A. D.; Finlayson-Pitts, B. J.; Gerber, R. B. Mechanism for Formation of Atmospheric Cl Atom Precursors in the Reaction of Dinitrogen Oxides with HCl/Cl⁻ on Aqueous Films. *Phys. Chem. Chem. Phys.* **2015**, *17* (29), 19360–19370. https://doi.org/10.1039/C5CP02664D.
- (31) Kercher, J. P.; Riedel, T. P.; Thornton, J. A. Chlorine Activation by N₂O₅: Simultaneous, in Situ Detection of ClNO₂ and N₂O₅ by Chemical Ionization Mass Spectrometry. *Atmos. Meas. Tech.* **2009**, *2* (1), 193–204. https://doi.org/10.5194/amt-2-193-2009.
- (32) Lee, B. H.; Lopez-Hilfiker, F. D.; Mohr, C.; Kurtén, T.; Worsnop, D. R.; Thornton, J. A. An Iodide-Adduct High-Resolution Time-of-Flight Chemical-Ionization Mass Spectrometer: Application to Atmospheric Inorganic and Organic Compounds. *Environ. Sci. Technol.* 2014, 48 (11), 6309–6317. https://doi.org/10.1021/es500362a.

- (33) Pegram, L. M.; Record, M. T. Hofmeister Salt Effects on Surface Tension Arise from Partitioning of Anions and Cations between Bulk Water and the Air–Water Interface. *J. Phys. Chem. B* **2007**, *111* (19), 5411–5417. https://doi.org/10.1021/jp070245z.
- (34) Bertram, T. H.; Thornton, J. A.; Riedel, T. P. An Experimental Technique for the Direct Measurement of N₂O₅ Reactivity on Ambient Particles. *Atmos. Meas. Tech.* **2009**, *2* (1), 231–242. https://doi.org/10.5194/amt-2-231-2009.
- (35) Osthoff, H. D.; Roberts, J. M.; Ravishankara, A. R.; Williams, E. J.; Lerner, B. M.; Sommariva, R.; Bates, T. S.; Coffman, D.; Quinn, P. K.; Dibb, J. E.; Stark, H.; Burkholder, J. B.; Talukdar, R. K.; Meagher, J.; Fehsenfeld, F. C.; Brown, S. S. High Levels of Nitryl Chloride in the Polluted Subtropical Marine Boundary Layer. *Nature Geosci.* 2008, 1 (5), 324–328. https://doi.org/10.1038/ngeo177.
- (36) Burkholder, J. B.; Sander, J. P.; Abbatt, J. P. D.; Barker, J. R.; Cappa, C. D.; Crounse, J. D.; Dibble, T. S.; Huie, R. E.; Kolb, C. E.; Kurylo, M. J.; Orkin, V. L.; Percival, C. J.; Wilmouth, D. M.; Wine, P. H. JPL Publication 19-5. Chemical Kinetics and Photochemical Data for Use in Atmospheric Studies; p 1610.
- (37) Royer, H. M.; Mitroo, D.; Hayes, S. M.; Haas, S. M.; Pratt, K. A.; Blackwelder, P. L.; Gill, T. E.; Gaston, C. J. The Role of Hydrates, Competing Chemical Constituents, and Surface Composition on ClNO₂ Formation. *Environ. Sci. Technol.* **2021**, *55* (5), 2869–2877. https://doi.org/10.1021/acs.est.0c06067.
- (38) Dörich, R.; Eger, P.; Lelieveld, J.; Crowley, J. N. Iodide CIMS and *m/z* 62: The Detection of HNO₃ as NO₃⁻ in the Presence of PAN, Peroxyacetic Acid and Ozone. *Atmos. Meas. Tech.* **2021**, *14* (8), 5319–5332. https://doi.org/10.5194/amt-14-5319-2021.
- (39) CRC Handbook of Chemistry and Physics; Rumble, J. R., Ed.; Taylor and Francis, 2021.

- (40) Sander, R. Compilation of Henry's Law Constants (Version 4.0) for Water as Solvent. *Atmospheric Chem. Phys.* **2015**, *15* (8), 4399–4981. https://doi.org/10.5194/acp-15-4399-2015.
- (41) Robinson, R. A.; Stokes, R. H. *Electrolyte Solutions, Second Revised Edition*; Dover Publications.
- (42) Virtanen, N.; Polari, L.; Välilä, M.; Mikkola, S. Kinetic Solvent Deuterium Isotope Effect in Transesterification of RNA Models. *J. Phys. Org. Chem.* **2005**, *18* (5), 385–397. https://doi.org/10.1002/poc.883.
- (43) Swain, C. G.; Evans, D. F. Conductance of Ions in Light and Heavy Water at 25°. *J. Am. Chem. Soc.* **1966**, 88 (3), 383–390. https://doi.org/10.1021/ja00955a001.
- (44) Vitagliano, V.; Lyons, P. A. Diffusion Coefficients for Aqueous Solutions of Sodium Chloride and Barium Chloride. *J. Am. Chem. Soc.* **1956**, 78 (8), 1549–1552. https://doi.org/10.1021/ja01589a011.
- (45) Bertram, T. H.; Cochran, R. E.; Grassian, V. H.; Stone, E. A. Sea Spray Aerosol Chemical Composition: Elemental and Molecular Mimics for Laboratory Studies of Heterogeneous and Multiphase Reactions. *Chem. Soc. Rev.* 2018, 47 (7), 2374–2400. https://doi.org/10.1039/C7CS00008A.